LA-UR- 11-05834

Approved for public release;
distribution is unlimited.

Title:	Simulation of polycrystalline aggregates to understand in-situ grain boundary stress states under dynamic loading conditions.
Author(s):	B.L. Hansen-T-3 C.A. Bronkhorst-T-3 I. Beyerlein-T-3 E.K. Cerreta-MST-8 D.Dennis-Koller- WX-9
Intended for:	Materials Science & Technology 2011 October 16-20, 2011 Columbus, Ohio USA

Form 836 (7/06)

Simulation of polycrystalline aggregates to understand in-situ grain boundary stress states under dynamic loading conditions

Thermal-mechanically coupled simulations of polycrystalline metallic materials were conducted using an elastic-viscoplastic slip based single crystal model with crystallographic orientation, temperature, and strain rate dependence. This model has been developed for use under both low and high rates of loading for copper. The microstructure of the polycrystalline aggregates were represented numerically by generating statistically equivalent topologies from experimentally quantified EBSD measurements on copper samples of varying characteristics. The simulations are conducted under both dynamic and shock loading conditions for materials which damage and fail by pore nucleation at grain boundaries. The simulation results are examined for intergranular relationships which could lead to pore nucleation conditions at grain boundaries under these states of loading. Where possible, comparisons are made between the simulation and matched experiments conducted on the material from which the microstructural statistics were drawn.

Simulation of polycrystalline aggregates to understand in-situ grain boundary stress states under dynamic loading conditions

BL Hansen, CA Bronkhorst, IJ Beyerlein
Theoretical Division, LANL
EK Cerreta
Material Science & Technology Division, LANL
D Dennis-Koller
Weapons Experiments Division, LANL

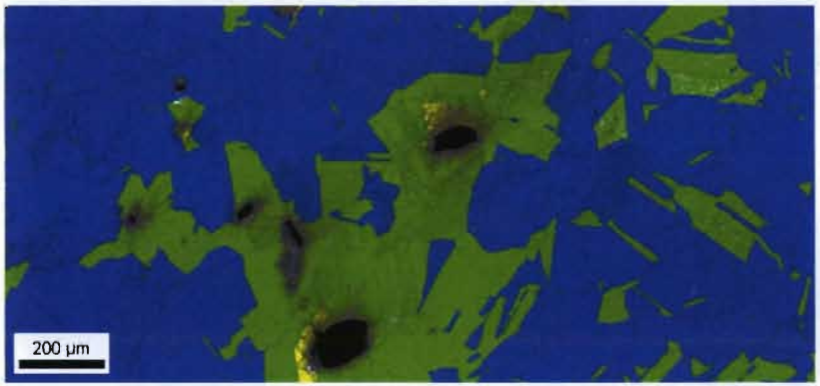

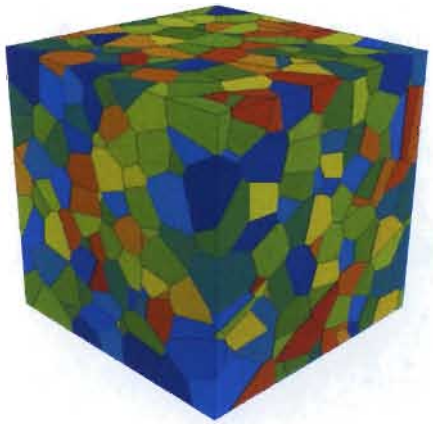

MS&T
Oct. 2011

LAUR 11-??????

Los Alamos NATIONAL LABORATORY EST. 1943

Strain Rates vary within Dynamic Experiments

In a dynamic experiment strain rates may vary by orders of magnitude.

Shock experiments reach strains of ~10^6 sec^{-1} consistently.

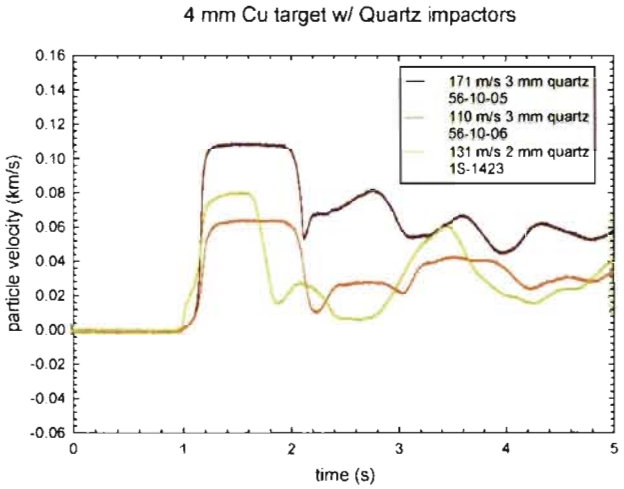

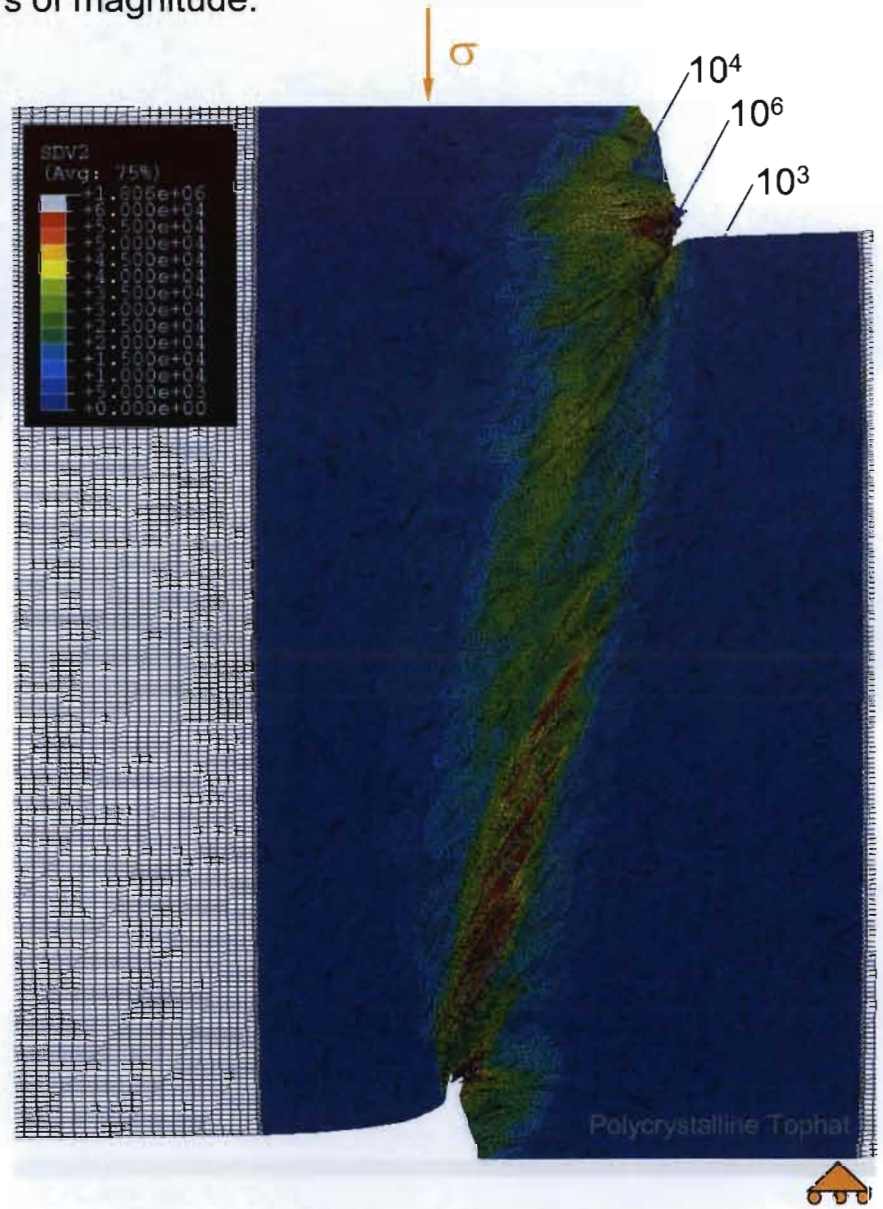

New Single Crystal Model for High Rates

$$\dot{\gamma}^{\alpha} = \dot{\gamma}_0 \exp\left[-\frac{F_0}{k\theta}\left\langle 1-\left\langle \frac{\left|\tau^{\alpha}\right| - s^{\alpha}\frac{\mu}{\mu_0}}{s_l^{\alpha}\frac{\mu}{\mu_0}}\right\rangle^{p}\right\rangle^{q}\right]\mathrm{sgn}\left(\tau^{\alpha}\right)$$

Previous model valid 10^4 or less

New single crystal model developed for strain rates exceeding the thermally activated range.

$$\dot{\gamma}_{\alpha} = b\rho_{\alpha}^{M} v_{\alpha} \qquad v_{\alpha} = \frac{\tau_{\alpha} b}{B}$$

$$\dot{\rho}_{\alpha}^{M} = \dot{\rho}_{\alpha}^{gen} + \dot{\rho}_{\alpha}^{prop} + \dot{\rho}_{P\alpha}^{esc} - \sum_{inter} \dot{\rho}_{M\alpha}^{inter}$$

New model valid through 10^6 and higher

10^4

Thermal Activated | Drag Dominated

Plastic flow behavior changes at a strain rate of ~10^4 sec^{-1}

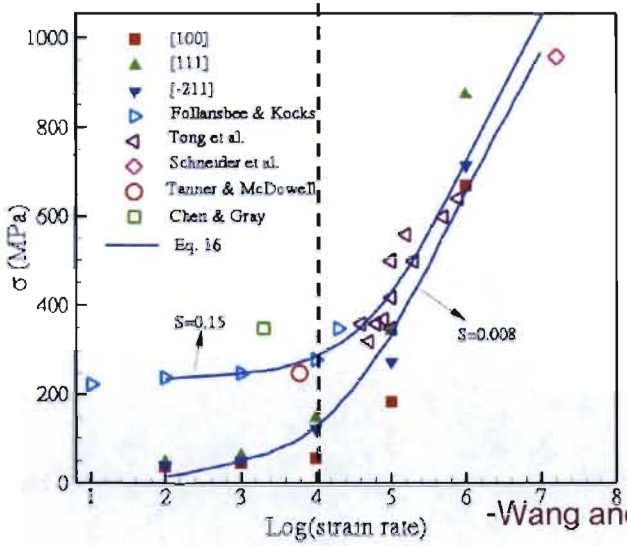

-Wang and Beyerlein

Based on modeling direct interaction of dislocations which improves validation.

Requisite Single Crystal Model

DOMAIN OF INTEREST

- Large deformation (plastic)
- Valid at high strain rates (10^6)
- Varying strain rates (spatial and temporal)
- Single crystal length scale (mesoscale)

GOALS OF CONSTITUTIVE MODEL

- Measureable physical parameters and state variables (i.e. dislocations)
- Includes strain rate sensitivities: quasi-static to shock-loaded with transition (latent hardening, kinetic effects, thermal effects)
- Crystalline microstructures directly represented
- Application to polycrystal shock loading, incorporation with damage

TA Tophat Shear (1357) E. Cerreta

Varying strain rates

Cu Plane Strain Compression

Undeformed $\varepsilon = -1.5$

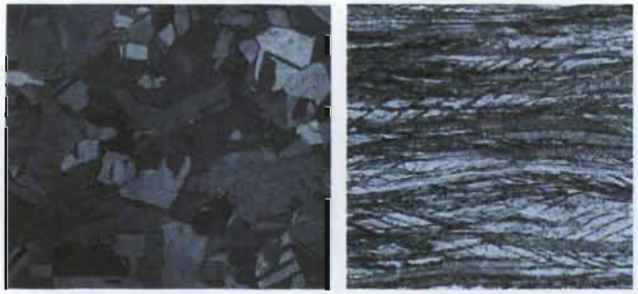

Large deformation

Localization from microstucture influences

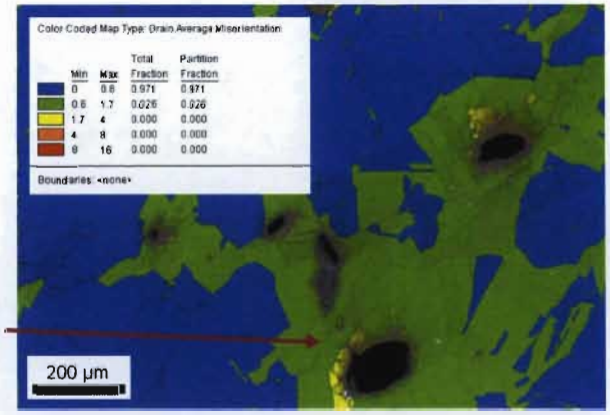

Regions adjacent to damage have above average strain

Directly model Dislocation Density

- Treat dislocation density as a state variable
- Determine a set of distinguishable statistical dislocation populations:
  - Mobile(ρ^M): glissile dislocations free to move and carry plasticity belonging to a slip system

$$inter^M = \{pile\ up, annihilate, sessile\ lock, no\ interaction\}$$

  - Pile-up(ρ^P): glissile dislocations belonging to a slip system which currently do not move due to being blocked by obstacles with a sufficient barrier to prevent motion

$$inter^P = \{escape, annihilate, sessile\ lock, no\ interaction\}$$

  - Debris(ρ^L): sessile obstacles to dislocation motion

  - Adaptable: edge and screw or other distinguishing features of dislocations could be included

Dislocation Interaction Rates

- Rate of interaction between each population is computed

$$\dot{\rho}_{AB}^{inter} = D_{AB}^{inter} \rho_B \rho_A |v_{AB}|$$

  - Thermal probability is required for certain interactions:

$inter$	$escape$	$trap$	$anni$	$lock$
$P_{A\alpha}^{inter}$	$\exp(esc_{A\alpha})$	$1-\exp(esc_{A\alpha})$	1	1

  - Depending on population types fractions may be required:

$$\rho_{B\beta} \Rightarrow f_{A\alpha B\beta}^{inter} \rho_{B\beta}$$

  - Total interaction:

$$\dot{\rho}_{A\alpha B\beta}^{inter} = c_{A\alpha B\beta}^{inter} P_{A\alpha}^{inter} D f_{A\alpha B\beta}^{inter} \rho_{B\beta} \rho_{A\alpha} |v_{A\alpha B\beta}|$$

  - Total interaction for a population is a sum:

$$\sum_{inter} \dot{\rho}_{A\alpha}^{inter} = \sum_{B} \sum_{\beta} \dot{\rho}_{A\alpha B\beta} = \sum_{inter} \sum_{B} \sum_{\beta} \dot{\rho}_{A\alpha B\beta}^{inter}$$

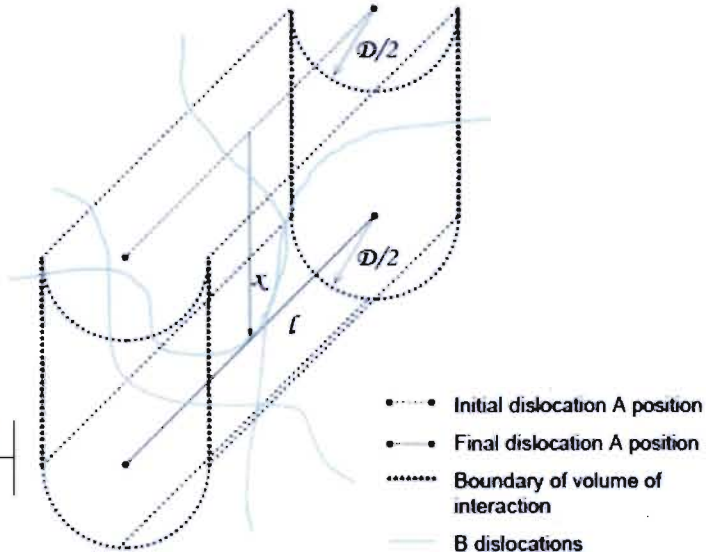

c is an accounting term: 2 if same population is interacting, 1 otherwise

Interaction Terms

Accounting Term

$$c_{AB}^{inter} = (1 + \delta_{M\alpha B\beta})(\delta_{(inter)(no)})$$

= 0, if no interaction

= 2, if same population

= 1, otherwise

Thermal Probability

$inter$	$escape$	$trap$	$anni$	$lock$
$P_{A\alpha}^{inter}$	$\exp(esc_{A\alpha})$	$1 - \exp(esc_{A\alpha})$	1	1

Table 3. Thermal probability of mobile dislocation interactions

$$\exp[esc_{A\alpha}] \equiv \exp\left[\frac{-((\tau_\alpha^G b - |\tau_\alpha|)b^2 - K_{A\alpha})\mathcal{L}}{k_b\theta}\right]$$

= 1, if interaction has no energy barrier

= 1, if stress and kinetic energy overcome barrier

0 < P < 1, otherwise

Fraction of Interactions

Defined by relation between slip systems and dislocation population types

	$f_{A\alpha B\beta}^{inter}$	$A = M$ $inter$				
		$lock$	$anni$	$pile$	no	
B	M, P self	0	0.5	0.5	0	$= 1$
	M, P collinear	0	0.5	0.5	0	
	M, P coplanar	0	0	0.5	0.5	
	M, P other	f^L	0	0	$1 - f^L$	
	L	0	0	1	0	

Table 1. Fraction of dislocation interactions for mobile dislocations

	$f_{A\alpha B\beta}^{inter}$	$A = P$ $inter$				
		$lock$	$anni$	esc	no	
B	M self	0	0.5	f^{esc}	1 - 0.5 - f^{esc}	$= 1$
	M collinear	0	0.5	f^{esc}	1 - 0.5 - f^{esc}	
	M coplanar	0	0	f^{esc}	1 - f^{esc}	
	M other	f^L	0	0	1 - f^L	

Table 2. Fraction of dislocation interactions for pile-up dislocations

Mobile Dislocations

- Generation – dislocation sources

$$\dot{\rho}_{\alpha}^{gen} = \rho_{\alpha}^{FR} f_{\alpha}^{act} R_{\alpha} l_{\alpha}^{FR}$$

$$\dot{\rho}_{\alpha}^{gen} = 4\pi \rho_{\alpha}^{FR} |v_{\alpha}^{M}| \exp\left[-2\pi \rho_{\alpha}^{FR} \left(\frac{2T}{\tau b}\right)^2\right]$$

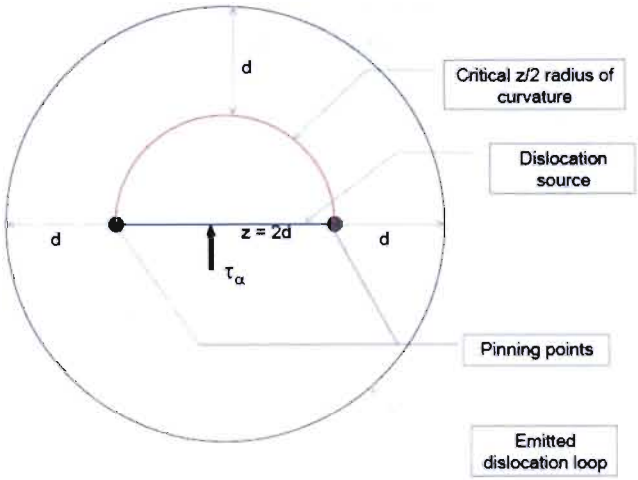

Based on random distribution of source pinning points

- Propagation – expansion of loops

$$\dot{\rho}_{\alpha}^{prop} = \dot{\bar{l}}_{\alpha} N_{\alpha}^{M} / \mathcal{V} = |v_{\alpha}| \rho_{\alpha}^{M} / \bar{r}_{\alpha}^{M}$$

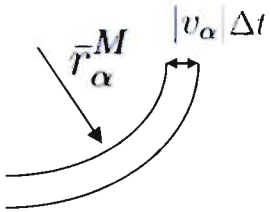

- Total – include thermal escape and interactions

$$\begin{aligned}\dot{\rho}_{\alpha}^{M} &= \dot{\rho}_{\alpha}^{gen} + \dot{\rho}_{\alpha}^{prop} + \dot{\rho}_{P\alpha}^{esc} - \sum_{inter} \dot{\rho}_{M\alpha}^{inter} \\ &= \dot{\rho}_{\alpha}^{gen} + \dot{\rho}_{\alpha}^{prop} + \dot{\rho}_{P\alpha}^{esc} - \sum_{B\beta} \left(\dot{\rho}_{M\alpha B\beta}^{lock} + \dot{\rho}_{M\alpha B\beta}^{pile} + \dot{\rho}_{M\alpha B\beta}^{anni}\right)\end{aligned}$$

Pile-up and Debris

- Thermal escape

$$\dot{\rho}_{P\alpha}^{esc\theta} = \frac{1}{k^{esc\theta}} \rho_{\alpha}^{P} \exp\left[esc_{P\alpha}\right]$$

Thermal fluctuation time constant

- Escape by collision

$$\dot{\rho}_{P\alpha M\beta}^{esc} = \exp[esc_{P\alpha}] D_{P\alpha M\beta}^{esc} f_{P\alpha M\beta}^{esc} \rho_{P\alpha} \rho_{M\beta} |v_{P\alpha M\beta}|$$

- Total

$$\begin{aligned} \dot{\rho}_{\alpha}^{P} &= \dot{\rho}_{M\alpha}^{pile} - \dot{\rho}_{P\alpha}^{esc\theta} - \sum \dot{\rho}_{P\alpha}^{inter} \\ &= \dot{\rho}_{M\alpha}^{pile} - \dot{\rho}_{P\alpha}^{esc\theta} - \sum_{\beta} \left(\dot{\rho}_{P\alpha M\beta}^{anni} + \dot{\rho}_{P\alpha M\beta}^{esc} + \dot{\rho}_{P\alpha M\beta}^{lock} \right) \end{aligned}$$

- Escape by stress path changes is in reversibility

- Debris $\dot{\rho}^{L} = \sum_{A\alpha} \sum_{B\beta} \dot{\rho}_{A\alpha B\beta}^{lock}$

Hardening and Kinetic Effects

- Mobile/Pile-up transition thermal probability
  - Obstacle density (determined by interactions and densities on other slip planes)
  - Latent hardening will be inherent
  - Kinetic effects are maintained

$$\exp[esc_{A\alpha}] \equiv \exp\left[\frac{-((\tau_\alpha^G b - |\tau_\alpha|)b^2 - K_{A\alpha})\mathcal{L}}{k_b\theta}\right]$$

Obstacle strength

$$\tau_\alpha^G = -\kappa\mu[\theta]b\sqrt{\rho_\alpha^I}\ln\left[b\sqrt{\rho_\alpha^I}\right] + s^L$$

Latent hardening: ρ_I function of all ρ

$$\rho_\alpha^I = \left(\frac{2}{\pi}\right)^2 \rho^L + \sum_\beta \frac{2}{\pi}\sqrt{1 - \mathbf{m}_\alpha \cdot \mathbf{m}_\beta}(\rho_\beta^M + \rho_\beta^P)$$

τ_α Applied shear stress to system α

$$K_{A\alpha} = \frac{1}{2}mv_{A\alpha}^2$$ Kinetic energy of dislocations $A\alpha$

Found to be relevant at $d\gamma/dt > 10^4$

High-rate to Low-rate Transition

- Transition between a thermally-activated system and a drag dominated system occurs:

$$\dot{\gamma}_\alpha = b\rho_\alpha^M v_\alpha$$

$$v_\alpha = \frac{\tau_\alpha b}{B}$$

$$\begin{aligned}\dot{\rho}_\alpha^M &= \dot{\rho}_\alpha^{gen} + \dot{\rho}_\alpha^{prop} + \dot{\rho}_{P\alpha}^{esc} + \sum_{inter} \dot{\rho}_{M\alpha}^{inter} \\ &= \dot{\rho}_\alpha^{gen} + \dot{\rho}_\alpha^{prop} + \dot{\rho}_{P\alpha}^{esc} + \sum_{B\beta} \left(\dot{\rho}_{M\alpha B\beta}^{lock} + \dot{\rho}_{M\alpha B\beta}^{pile} + \dot{\rho}_{M\alpha B\beta}^{anni} \right)\end{aligned}$$

Competition between rate of escape of pile-ups and rate of pile-up of mobile dislocations.

Slip Rate for Single Slip System

Conditions

- Fixed density of obstacles:
  ρ^I = constant
- Fixed total density of dislocations:
  $\rho^M+\rho^P$ = constant
- Impose a strain rate (equivalent to slip rate), compute shear stress required by iteration

Single Slip System
Imposed Strain Rate

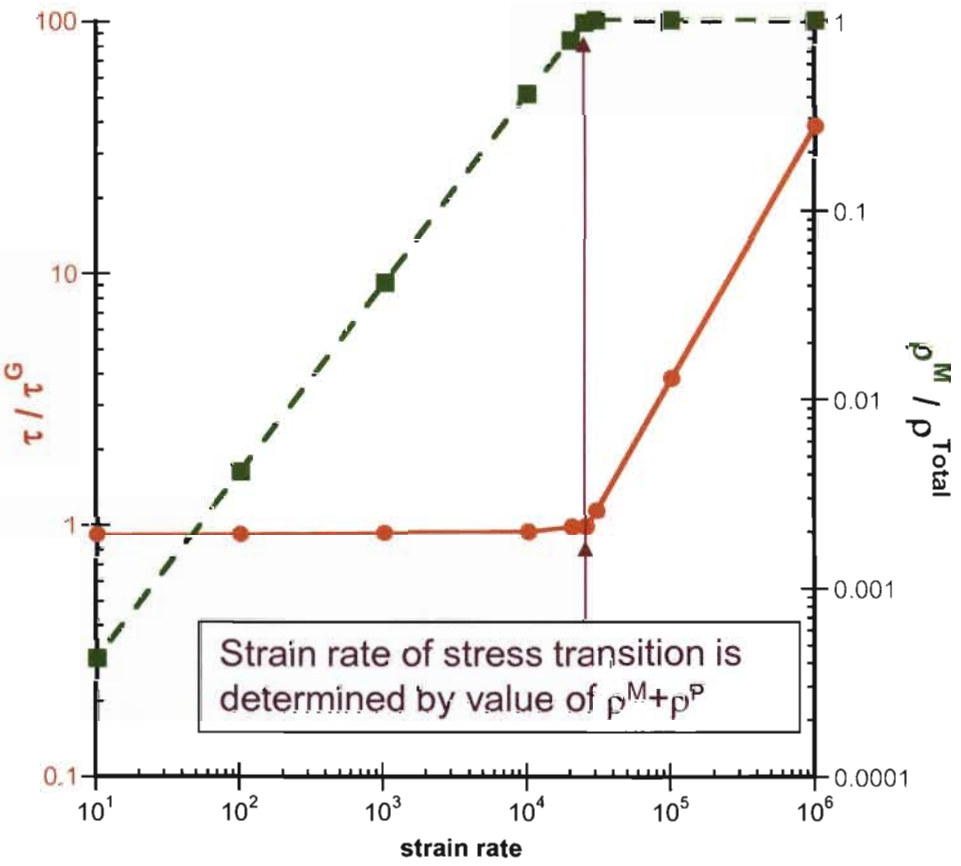

•Transition between thermally-activated and drag dominated evident.
•Comparable to polycrystalline experiments and d.d. simulations.

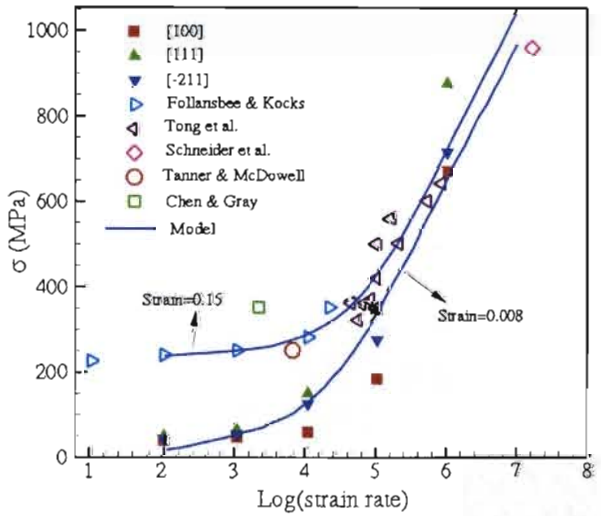

Boundary Conditions

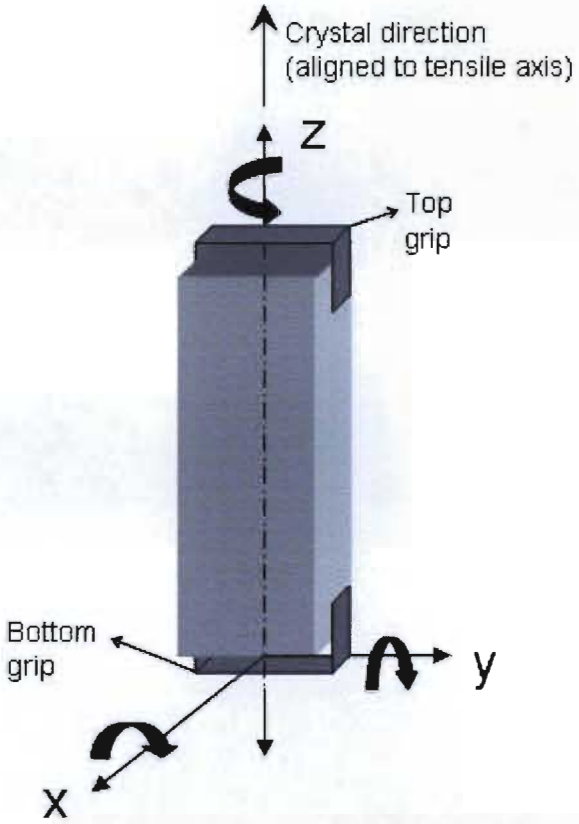

$$F = \begin{pmatrix} ? & 0 & 0 \\ 0 & ? & 0 \\ 0 & 0 & f \end{pmatrix}$$

$$P = \begin{pmatrix} 0 & ? & ? \\ ? & 0 & ? \\ ? & ? & ? \end{pmatrix}$$

Table 4.1: Copper Material Constants

Constant	Value	Ref.
Elastic Const. (C_{11})	168.4 GPa	[GH71]
Elastic Const. (C_{12})	121.4 GPa	[GH71]
Elastic Const. (C_{44})	75.4 GPa	[GH71]
Crit. Shear Stress (τ^c)	1.0 MPa	[Bar52]
Burgers Vector (b)	$2.56 * 10^{-}10$ m	[KAA75]
Line Tension (T)	$18.3 * 10^{-}10$ N	[KAA75]

Single Crystal Tension Results

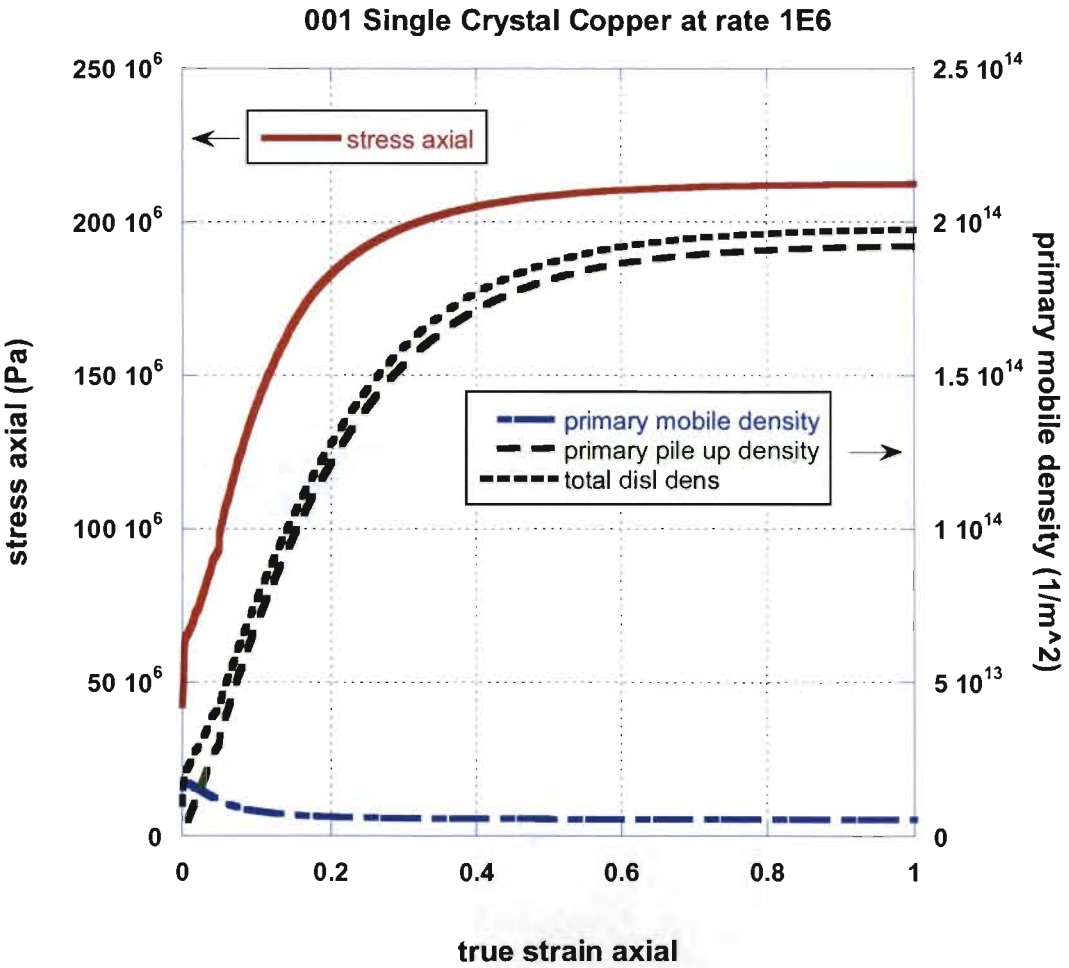

Run of a full single crystal material point

- Stresses from elastic model.
- Implicit integration.
- Strain rate of 1.
- Densities for one of the 8 primary slip systems displayed.
- Due to symmetry 8 primary slip planes are identical.

Experimental Comparison

Rate Dependent Flow Stress of Copper

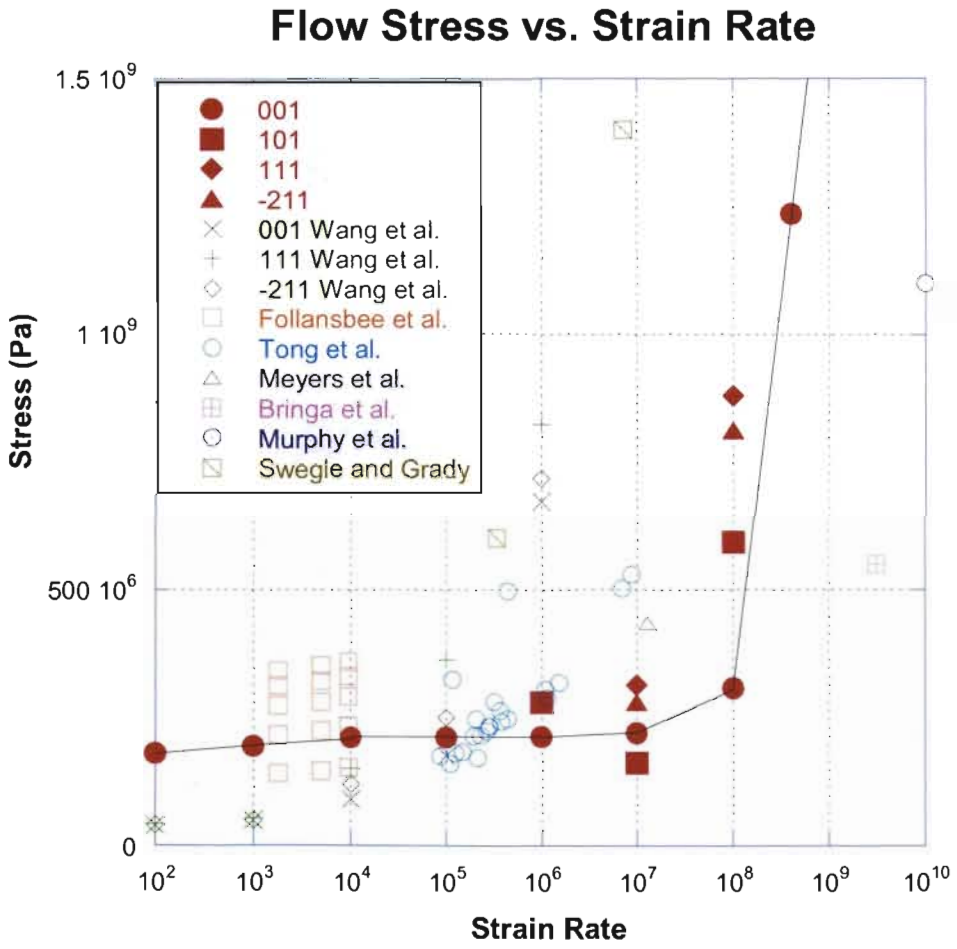

Source	Type	Material
Wang et al.	DD simulation	Various single crystals
Follansbee et al.	Hopkinson bar	Polycrystal
Tong el al.	Impact shear shocked	Polycrystal
Meyers et al.	Laser shocked	001 single crystal
Bringa et al.	MD simulation	001 single crystal
Murphy et al.	Laser shocked	001 single crystal
Swegle and Grady	Impact shocked	Polycrystal

Rate Comparison

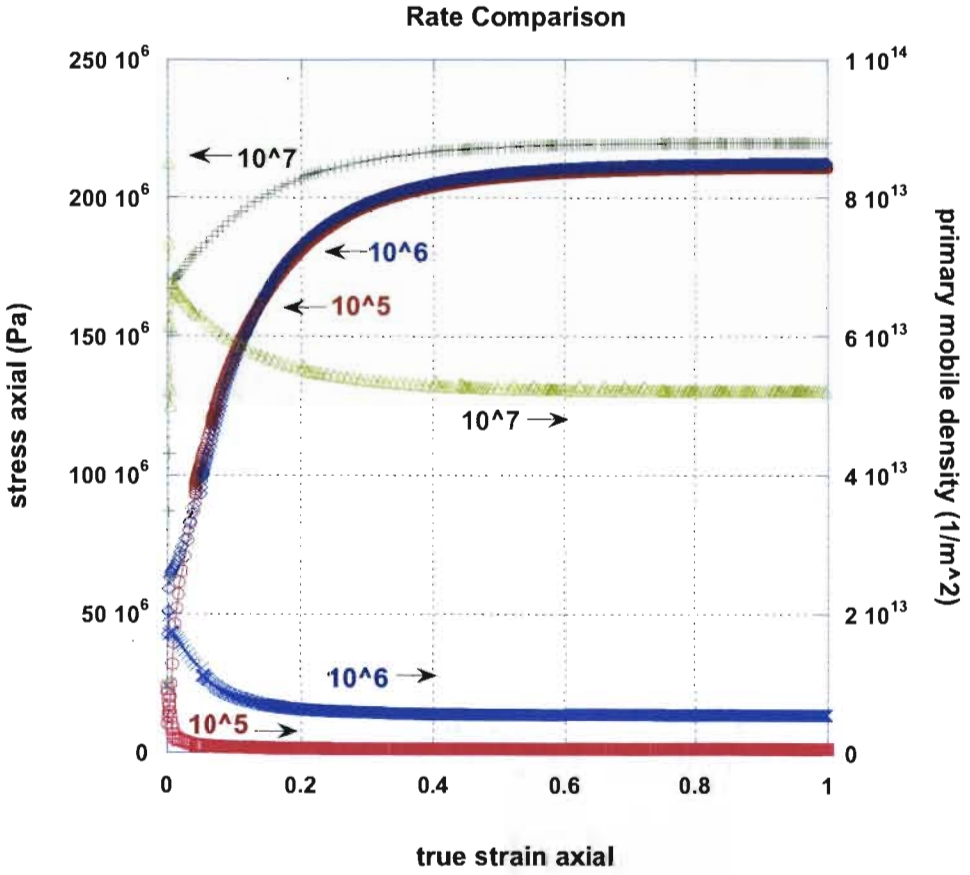

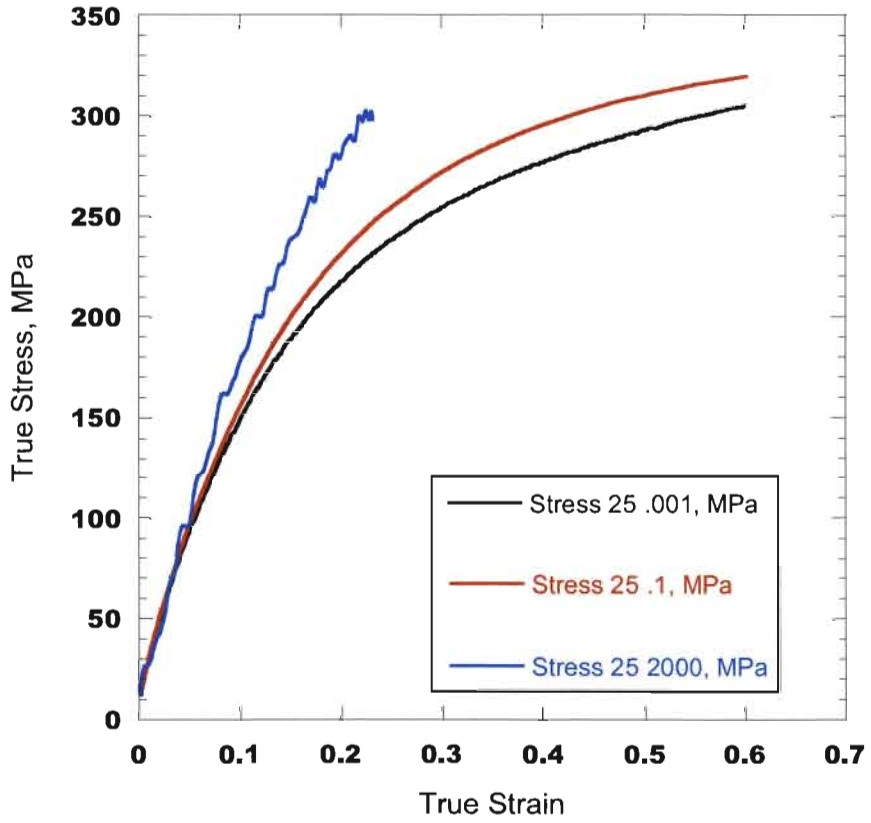

Note, stress scales
and rates are different

Temperature Comparison

Temperature Dependent Flow Stress of Copper

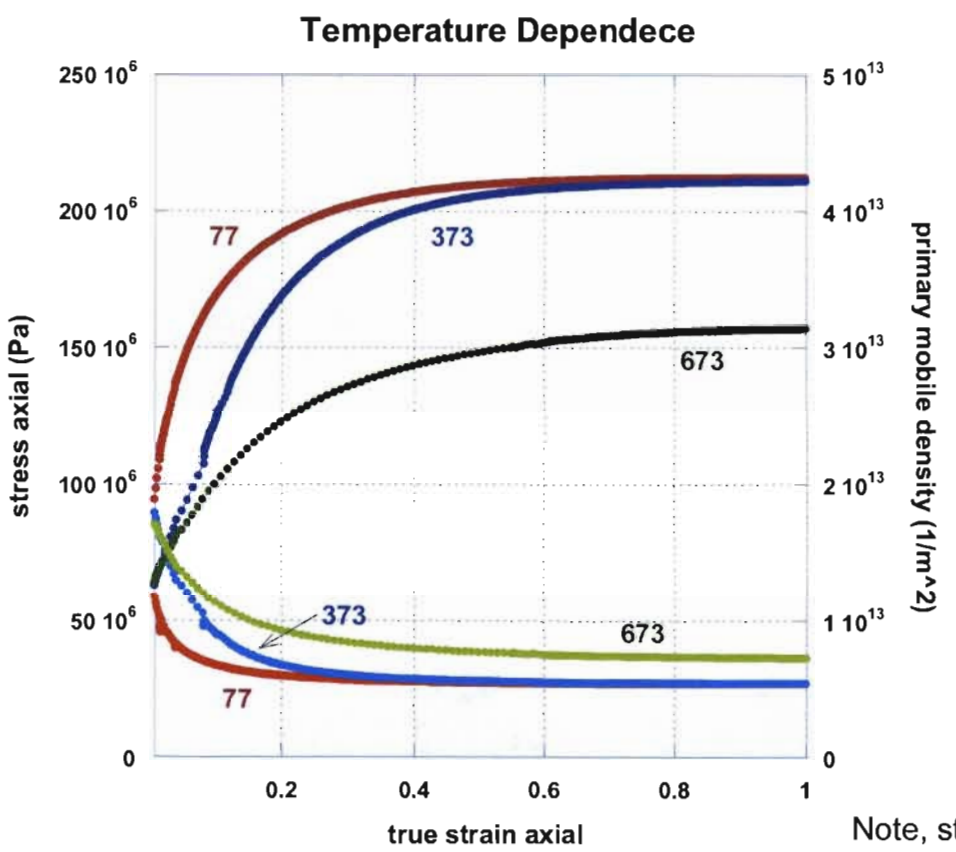

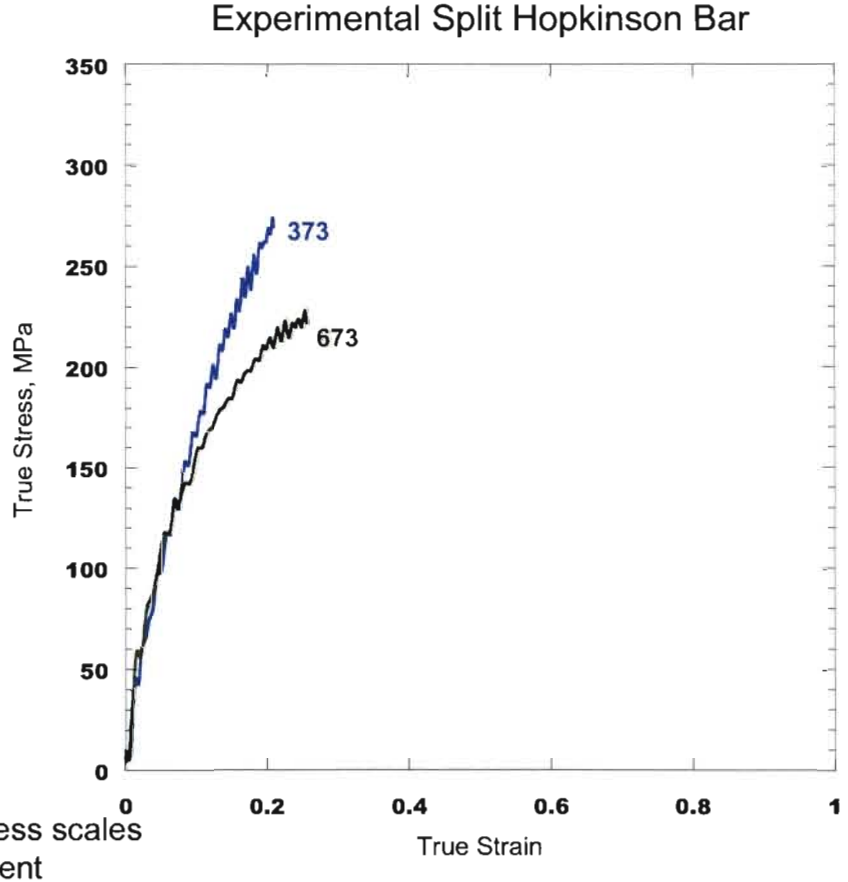

Note, stress scales are different

Highlights of New Dislocation-based Plasticity Model

- Dislocation densities modeled directly for comparison to experimental quantities.
- Physical parameters
- Easily adjustable dislocation populations interactions – for varying materials.
- Inherent transition from high-rate drag-dominated to low-rate thermally activated dislocation motion.
- Includes kinetic effects, latent hardening, and thermal softening.
- Statistical representation of dislocation evolution.

Current focus on FCC materials.

Challenge of linking microstructure to performance

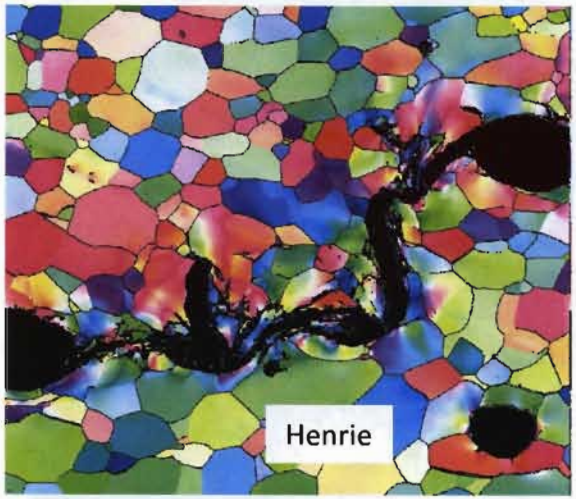

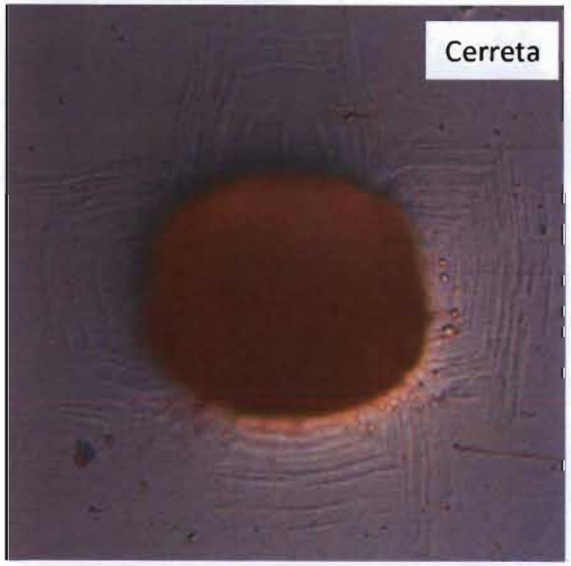

- The large deformation (strains of 3.0)/high rate (10^6 sec^{-1}) ductile failure process generally involves localization, porosity initiation, porosity growth, and coalescence dominated by localized deformation.
- These physical events are stochastic, occur over several length scales, and intimately involves the microstructure.
- Understanding these complex thermo-mechanical processes is critical to our ability to numerically represent and predict large deformation and damage / failure events.